A Heterodinuclear $Co^{II}Cu^{I}$ Complex with Co(salen) in a Macrocyclic Framework. Oxygenation Studies in Comparison with Analogous $Cu^{II}Cu^{I}$ and $Co^{II}Pb^{II}$ Complexes

Misato Shinoura, Satoru Kita, Masaaki Ohba, and Hisashi Ōkawa*

Department of Chemistry, Faculty of Science, Kyushu University, Hakozaki, Higashiku 6-10-1, Fukuoka 812-8581, Japan

Hideki Furutachi and Masatatsu Suzuki

Department of Chemistry, Faculty of Science, Kanazawa University, Kakuma-machi, Kanazawa, 920-1192, Japan

Received March 20, 2000

A di(μ-phenoxo)$Co^{II}Cu^{I}$ complex, $[CoCu(L)]ClO_4 \cdot 0.5DMF$, has been prepared where $(L)^{2-}$ is a macrocyclic dinucleating compartmental ligand derived from the 2:1:1 condensation of 2,6-diformyl-4-methylphenol, ethylenediamine, and 3-thia-1,5-pentanediamine, having a salen-like N_2O_2 metal-binding site (salen = *N*,*N*′-ethylenedisalicylideneaminate) and an N_2O_2S site sharing the phenolic oxygens. It crystallizes in the monoclinic space group $P2_1/n$, $a = 7.087(1)$ Å, $b = 19.593(6)$ Å, $c = 19.447(3)$ Å, $\beta = 96.29(1)°$, $V = 2684(1)$ Å^3, and $Z = 4$. The Co^{II} resides in the salen-like site and assumes a planar geometry. The Cu^{I} in the N_2O_2S site has a planar four-coordinate geometry with two phenolic oxygens and two imine nitrogens; the thioether sulfur on the lateral chain is situated at an axial site of the Cu^{I}, but the Cu--S separation is very large (3.08 Å). In the $\{CuN_2O_2\}$ chromophore, the two Cu−O bond distances (2.333(5) and 2.385(5) Å) are significantly long relative to the two Cu−N bond distances (1.984(6) and 1.929(4) Å). Further, the N−Cu−N angle is very large (128.2(2)°), whereas the O−Cu−O angle is very small (65.2(2)°). Analogous $Cu^{II}Cu^{I}$ and $Co^{II}Pb^{II}$ complexes of $(L)^{2-}$, $[Cu^{II}Cu^{I}(L)]ClO_4$ and $[CoPb(L)](ClO_4)_2$, have been prepared. The DMF adduct of $[Cu^{II}Cu^{I}(L)]ClO_4$, $[Cu^{II}Cu^{I}(L)]ClO_4 \cdot 0.5DMF$, crystallizes in the monoclinic space group $P2_1/n$, $a = 6.957(2)$ Å, $b = 23.774(2)$ Å, $c = 7.758(3)$ Å, $\beta = 94.72(3)°$, $V = 1278.8(6)$ Å^3, and $Z = 4$. The dinuclear core resembles that of the $Co^{II}Cu^{I}$ complex and shows distortions about the Cu^{I} similar to those found for the $Co^{II}Cu^{I}$ complex. The di-DMF adduct of the $Co^{II}Pb^{II}$ complex, $[CoPb(L)(DMF)_2](ClO_4)_2$, crystallizes in the monoclinic space group $P2_1/n$, $a = 16.265(2)$ Å, $b = 12.640(2)$ Å, $c = 18.584(3)$ Å, $\beta = 90.43(1)°$, $V = 3820.5(8)$ Å^3, and $Z = 4$. The Co^{II} in the N_2O_2 site has a square-pyramidal geometry together with a DMF oxygen at the apical site. The Pb^{II} in the N_2O_2S site has a six-coordinate geometry with the further coordination of a DMF molecule. The reactivity of the $Co^{II}Cu^{I}$ complex toward dioxygen has been studied in comparison with the $Cu^{II}Cu^{I}$ and $Co^{II}Pb^{II}$ complexes. The $Co^{II}Cu^{I}$ complex in DMF is very sensitive to dioxygen and is oxidized at −50 °C. The $Cu^{II}Cu^{I}$ complex is inert to dioxygen. The $Co^{II}Pb^{II}$ complex is oxygenated at 0 °C to form a peroxo dimer ($Pb^{II}Co^{III}-O-O-Co^{III}Pb^{II}$). The high sensitivity of the $Co^{II}Cu^{I}$ complex to dioxygen is explained by the irreversible oxidation to a $Co^{III}Cu^{II}$ species through an intramolecular-type peroxo complex ($Co^{III}-O-O-Cu^{II}$).

Introduction

Heterodinuclear cores were recently recognized at active sites of some metalloenzymes such as purple acid phosphatase (FeZn),[1] human calcineurin (FeZn),[2] and human protein phosphatase 1 (MnFe).[3] Another recent topic of heterobimetallic biosites is the heme a_3/Cu_B center at the terminus of the respiratory chain where an iron/copper pair catalyzes the dioxygen reduction into water together with heme *a* and Cu_A.[4] These findings have stimulated interest in functions associated with an interplay of dissimilar metal ions in close proximity. However, heterodinuclear complexes have been poorly studied for their functions because they often cause decomposition or metal scrambling in solution.

In order to provide discrete and stable heterodinuclear complexes, it is recommended to use dinucleating compartmental ligands whose two metal-binding sites are not equivalent with respect to the cavity size, the coordination number, or the nature of donor atoms.[5] Macrocyclic compartmental ligands in Chart 1 have been developed in this laboratory for this purpose.[6−8] Our recent interest using these macrocycles is to

(1) Strater, N.; Klabunde, T.; Tucker, P.; Witzel, H.; Krebs, B. *Science* **1995**, *268*, 1489.
(2) Kissinger, C. R.; Parge, H. E.; Knighton, D. R.; Lewis, C. T.; Pelletier, L. A.; Tempczyk, A.; Kalish, V. J.; Tucker, K. D.; Showalter, R. E.; Moomaw, E. W.; Gastinel, L. N.; Habuka, N.; Chen, X.; Maldonado, F.; Barker, J. E.; Bacquet, R.; Villafranca, E. *Nature* **1995**, *378*, 641.
(3) Engloff, M.-P.; Cohen, P. T. W.; Reinemer, P.; Barford, D. *J. Mol. Biol*. **1995**, *254*, 942.
(4) (a) Babcok, G. T.; Wikstrom, M. *Nature* **1992**, *356*, 301. (b) Malmstrom, B. G. *Acc. Chem. Res*. **1993**, *26*, 332. (c) Kitagawa, T.; Ogura, T. *Prog. Inorg. Chem*. **1997**, *45*, 431.
(5) Ōkawa, H.; Furutachi, H.; Fenton, D. E. *Coord. Chem. Rev.* **1998**, *174*, 51.
(6) (a) Wada, H.; Motoda, K.; Ohba, M.; Sakiyama, H.; Matsumoto, N.; Okawa, H. *Bull. Chem. Soc. Jpn*. **1995**, *68*, 1105. (b) Wada, H.; Aono, T.; Motoda, K.; Ohba, M.; Matsumoto, N.; Ōkawa, H. *Inorg. Chim. Acta* **1996**, *246*, 13. (c) Aono, T.; Wada, H.; Aratake, Y.; Matsumoto,

10.1021/ic000305e CCC: $19.00
Published on Web 09/01/2000

Chart 1. Chemical Structures of Macrocyclic Ligands

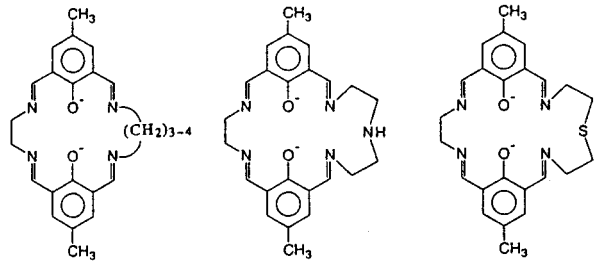

provide heterobimetallic systems of functional significance. Heterodinuclear complexes possessing Co(salen) as one complex entity in the macrocyclic framework are of particular interest because Co(salen) and its analogues are known for their reactivity toward dioxygen[9] (salen = *N*,*N*′-ethylenedisalicylideneaminate). In our recent studies on oxygenation of such $Co^{II}M^{II}$ complexes,[10,11] an intermolecular peroxo dimer ($M^{II}Co^{III}-O-O-Co^{III}M^{II}$) is generally produced, but an intramolecular peroxo complex is also formed depending upon the nature of the adjacent metal ion and the dinuclear core structure.

Our aim in this work is to prepare analogous $Co^{II}Cu^{I}$ complexes and to examine their reactivity toward dioxygen. The macrocyclic ligand of type C (abbreviated as H_2L) is adopted because the sulfur donor atom introduced into one lateral chain stabilizes Cu^{I} at the N_2O_2S site to form a $Cu^{II}Cu^{I}$ complex, $[Cu^{II}Cu^{I}(L)]ClO_4$.[8] The $Co^{II}Cu^{I}$ and $Co^{II}Pb^{II}$ complexes, $[CoCu(L)]ClO_4 \cdot 0.5DMF$ and $[CoPb(L)](ClO_4)_2$, are prepared by the stepwise template reaction. The X-ray crystallographic studies for $[CoCu(L)]ClO_4 \cdot 0.5DMF$ and $[Cu^{II}Cu^{I}(L)]ClO_4 \cdot 0.5DMF$ (crystallized from DMF in this work) have indicated a rare coordination geometry about the Cu^{I}. The focus is placed on oxygenation of $[CoCu(L)]ClO_4 \cdot 0.5DMF$ in comparison with $[Cu^{II}Cu^{I}(L)]ClO_4$ and $[CoPb(L)](ClO_4)_2$.

Experimental Section

Physical Measurements. Elemental analyses of C, H, and N were obtained at The Service Center for Elemental Analysis of Kyushu University. Metal analyses were performed on a Shimadzu AA-680 atomic absorption/flame emission spectrophotometer. Infrared spectra were recorded on a Perkin-Elmer BX FT-IR system using KBr disks. Electronic absorption spectra were recorded on a Shimadzu UV-3100PC spectrophotometer. Molar conductances were measured with a DKK AOL-10 conductivity meter at room temperature. X-Band ESR spectra were recorded on a JEOL JEX-FE3X spectrometer. Cyclic voltammograms were measured using a BAS CV-50W electrochemical analyzer in DMF solution containing tetra(*n*-butyl)ammonium perchlorate (TBAP) as the supporting electrolyte (**CAUTION!** TBAP is explosive and should be handled with great care). A three-electrode cell was used which was equipped with a glassy carbon working electrode, a platinum coil as the counter electrode, and a Ag/Ag^{+} (TBAP/acetonitrile) reference electrode.

Preparation. *N*,*N*′-Di(3-formyl-5-methylsalicylidene)ethylenediaminatocobalt(II) was prepared by a literature method.[12] All operations for synthesizing the $Co^{II}Cu^{I}$ and $Co^{II}Pb^{II}$ complexes were carried out in an atmosphere of nitrogen using a glovebox from Vacuum Atmospheres Company, Model MO-40-IV, or in an atmosphere of argon using a standard Schlenk apparatus to avoid oxidation by atmospheric dioxygen. The synthesis of $[Cu^{II}Cu^{I}(L)]ClO_4$ was reported previously.[8]

$[CoCu(L)]ClO_4 \cdot 0.5DMF$. To a suspension of *N*,*N*′-di(3-formyl-5-methylsalicylidene)ethylenediaminatocobalt(II) (123 mg, 0.3 mmol) in acetonitrile (50 cm^3) was added an acetonitrile solution (10 cm^3) of $[Cu(CH_3CN)_4]ClO_4$ (98 mg, 0.3 mmol), and the mixture was stirred for 3 h to form an orange solution. An acetonitrile solution of 3-thia-1,5-pentanediamine (36 mg, 0.3 mmol) was dropwise added, and the mixture was stirred at the boiling temperature for 1 h. The resulting red solution was evaporated to dryness, the residue was dissolved in DMF (10 cm^3), and the solution was diffused with 2-propanol (ca. 20 cm^3) to give red needles. Yield: 130 mg (65%). Anal. Found: C, 44.31; H, 4.09; N, 8.79; Co, 8.89. Calcd for $C_{25.5}H_{29.5}ClCoCuN_{4.5}O_{6.5}S$: C, 44.19; H, 4.29; N, 9.09; Co, 8.50. Selected IR data [ν/cm^{-1}] using KBr disks: 2903, 2855, 1632, 1088, 622. Molar conductance [Λ_M/S cm^2 mol^{-1}]: 58 in DMF.

$[CoPb(L)](ClO_4)_2$. To a suspension of *N*,*N*′-di(3-formyl-5-methylsalicylidene)ethylenediaminatocobalt(II) (820 mg, 2 mmol) in methanol (30 cm^3) was added a methanol solution (5 cm^3) of $Pb(ClO_4)_2 \cdot 3H_2O$ (920 mg, 2 mmol), and the mixture was stirred for 30 min to form an orange solution. To this was added a solution of 3-thia-1,5-pentanediamine (240 mg, 2 mmol) in methanol (10 cm^3) dropwise, and the mixture was stirred at the reflux temperature for 3 h to give an orange precipitate. It was recrystallized from DMF as orange crystals. Yield: 76%. Anal. Found: C, 32.23; H, 3.11; N, 6.11; Co, 6.14. Calcd for $C_{24}H_{26}Cl_2CoN_4O_{10}PbS$: C, 32.04; H, 2.91; N, 6.23; Co, 6.55. Selected IR data [ν/cm^{-1}] using KBr disks: 2924, 2858, 1619, 1110, 1060, 624. Molar conductance [Λ_M/S cm^2 mol^{-1}]: 106 in DMF.

Recrystallization from DMF formed $[CoPb(L)(DMF)_2](ClO_4)_2$ as good crystals suitable for X-ray crystallography.

Single-Crystal X-ray Analyses. The structure analysis for $[CoCu(L)]ClO_4 \cdot 0.5DMF$ was done on a Rigaku RAXIS-IV imaging plate area detector using graphite-monochromated Mo Kα radiation ($\lambda = 0.71070$ Å) at −120 °C. A single crystal was mounted on a glass fiber and coated with epoxy resin. In order to determine the cell constants and the orientation matrix, three oscillation photographs were taken with an oscillation angle of 2° and an exposure time of 10 min for each frame. Intensity data were collected by taking oscillation photographs (total oscillation range 132°, 46 frames, oscillation angle 3°, and exposure time 18 min). The data were corrected for Lorentz and polarization effects but not for absorption effect.

The structures of $[CoPb(L)(DMF)_2](ClO_4)_2$ and $[Cu^{II}Cu^{I}(L)]ClO_4 \cdot 0.5DMF$ were analyzed with a Rigaku AFC7R diffractometer with graphite-monochromated Mo Kα radiation ($\lambda = 0.71069$ Å) and a 12 kW rotating anode generator. Each single crystal was mounted on a glass fiber and coated with epoxy resin. The data were collected using an $\omega-2\theta$ scan technique to a maximum 2θ value of 50.0° at a scan speed of 16.0°/min (in ω). The weak reflections ($I < 10.0\sigma(I)$) were rescanned (maximum of four scans), and the counts were accumulated to ensure good counting statistics. Stationary background counts were recorded on each side of the reflection. The ratio of peak counting

N.; Ōkawa, H.; Matsuda, Y. *J. Chem. Soc., Dalton Trans*. **1996**, 25. (d) Ōkawa, H.; Aratake, Y.; Motoda, K.; Ohba, M.; Sakiyama, H.; Matsumoto, N. *Supramol. Chem.* **1996**, *6*, 293. (e) Aono, T.; Wada, H.; Yonemura, M.; Ohba, M.; Ōkawa, H.; Fenton, D. E. *J. Chem. Soc., Dalton Trans*. **1997**, 1527. (f) Aono, T.; Wada, H.; Yonemura, M.; Furutachi, H.; Ohba, M.; Ōkawa, H. *J. Chem. Soc., Dalton Trans*. **1997**, 3029.

(7) (a) Ōkawa, H.; Nishio, J.; Ohba, M.; Tadokoro, M.; Matsumoto, N.; Koikawa, M.; Kida, S.; Fenton, D. E. *Inorg. Chem*. **1993**, *32*, 2949. (b) Nishio, J.; Ōkawa, H.; Ohtsuka, S.; Tomono, M. *Inorg. Chim. Acta* **1994**, *218*, 27.

(8) Otsuka, S.; Kodera, M.; Motoda, K.; Ohba, M.; Okawa, H. *J. Chem. Soc., Dalton Trans*. **1995**, 2599.

(9) (a) McLendon, G.; Martell, A. E. *Coord. Chem. Rev*. **1976**, *19*, 1. (b) Jones, R. D.; Summerville, D. A.; Basolo, F. *Chem. Rev*. **1979**, *79*, 139. (c) Smith, T. D.; Pilbow, J. R. *Coord. Chem. Rev*. **1981**, *39*, 295. (d) Niederhoffer, E. C.; Timmons, J. H.; Martell, A. E. *Chem. Rev*. **1984**, *84*, 137.

(10) (a) Shimoda, J.; Furutachi, H.; Yonemura, M.; Ohba, M.; Matsumoto, N.; Ōkawa, H. *Chem. Lett*. **1996**, 979. (b) Furutachi, H.; Fujinami, S.; Suzuki, M.; Ōkawa, H. *Chem. Lett*. **1998**, 779. (c) Furutachi, H.; Ishida, A.; Miyasaka, H.; Ohba, M.; Fukita, N.; Ōkawa, H.; Koikawa, M. *J. Chem. Soc., Dalton. Trans.* **1999**, 367. (d) Furutachi, H.; Fujinami, S.; Suzuki, M.; Ōkawa, H. *Chem. Lett*. **1999**, 763. (e) Furutachi, H.; Fujinami, S.; Suzuki, M.; Ōkawa, H. *J. Chem. Soc., Dalton Trans*. **1999**, 2197.

(11) Kita, S.; Furutachi, H.; Ōkawa, H. *Inorg. Chem*. **1999**, *38*, 4038.

(12) Furutachi, H.; Ōkawa, H. *Inorg. Chem*. **1997**, *36*, 3911.

Table 1. Crystallographic Data for $[CoCu(L)]ClO_4 \cdot 0.5DMF$, $[Cu^{II}Cu^{I}(L)]ClO_4 \cdot 0.5DMF$ and $[CoPb(L)(DMF)_2](ClO_4)_2$

	$CoCu^{I}$	$Cu^{II}Cu^{I}$	CoPb
fw	693.03	512.41	557.92
temp/°C	−120	20	20
cryst syst	monoclinic	monoclinic	monoclinic
space group	$P2_1/n$ (No.14)	$P2_1$ (No. 4)	$P2_1/n$ (No. 14)
a/Å	7.087(1)	6.957(2)	16.265(2)
b/Å	19.593(6)	23.774(2)	12.640(2)
c/Å	19.447(3)	7.758(3)	18.584(2)
β/deg	96.29(1)	94.72(3)	90.431(9)
V/Å^3	2684.1(1)	1278.8(6)	3820.5(8)
Z	4	2	4
D_c/g cm^{-3}	1.715	1.717	1.635
μ(Mo Kα)/cm^{-1}	16.41	18.98	51.04
no. of reflns ($I > 3\sigma(I)$)	4783	3234	9478
R^a	0.044	0.032	0.042
$R_w{}^b$	0.049	0.041	0.033

^{a} $R = \Sigma||F_o| - |F_c||/\Sigma|F_o|$. ^{b} $R_w = [(\Sigma(|F_o| - |F_c|)^2/\Sigma F_o^2]^{1/2}$.

time to background counting time was 2:1. The diameter of the incident beam collimator was 1.0 mm, the crystal-to-detector distance was 235 mm, and the computer-controlled detector aperture was set to 9.0 × 13.0 mm (horizontal × vertical). The intensities of three representative reflections were measured after every 150 reflections. Over the course of the data collection, the standard reflections were monitored, and the decay corrections were applied by a polynomial correction An empirical absorption correction based on azimuthal scans of several reflections was applied. The data were corrected for Lorentz and polarization effects.

All of the structures were solved by the direct method and expanded using Fourier techniques. The non-hydrogen atoms were refined anisotropically. Hydrogen atoms were included in the structure factor calculation but not refined. Full-matrix least-squares refinements were based on observed reflections with $I > 3.00\sigma(I)$. The unweighted and weighted agreement factors were defined as $R = \Sigma||F_o| - |F_c||/\Sigma|F_o|$ and $R_w = [\Sigma w(|F_o| - |F_c|)^2/\Sigma w|F_o|^2]^{1/2}$. Plots of $\Sigma w(|F_o| - |F_c|)^2$ vs $|F_o|$, reflection order in data collection, $\sin\theta/\lambda$, and various classes of indices showed no unusual trends. Crystal data and details of the structure determinations are summarized in Table 1.

Neutral atom scattering factors were taken from Cromer and Waber.[13] Anomalous dispersion effects were included in F_{calc};[14] the values $\Delta f'$ and $\Delta f''$ were those of Creagh and McAuley.[15] The values for the mass attenuation coefficients are those of Creagh and Hubbel.[16] All calculations were performed on an IRIS Indigo computer using the teXsan[17] crystallographic software package from the Molecular Structure Corporation.

Results and Discussion

Preparation and General Characterization. In our previous study,[8] the mononuclear Cu^{II} complex, $[Cu(H_2L)](ClO_4)_2$, was prepared by a template reaction and used for the synthesis of the $Cu^{II}Cu^{I}$ complex $[Cu^{II}Cu^{I}(L)]ClO_4$. The corresponding macrocyclic mononuclear Co^{II} complex, however, could not be obtained by a similar template reaction. Thus, the acyclic proligand complex, *N*,*N*′-di(3-formyl-5-methylsalicylidene)ethylenediaminatocobalt(II), was reacted with 3-thia-1,5-pentanediamine in the presence of Cu^{I} to obtain the $Co^{II}Cu^{I}$ complex, $[CoCu(L)]ClO_4 \cdot 0.5DMF$. Similarly, $[CuPb(L)](ClO_4)_2$ was obtained by the reaction of *N*,*N*′-di(3-formyl-5-methylsalicylidene)-ethylenediaminatocobalt(II) with 3-thia-1,5-pentanediamine in the presence of Pb^{II} in methanol.

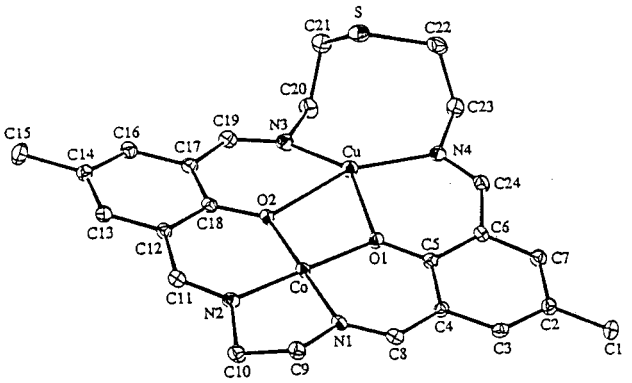

Figure 1. ORTEP view of $[CoCu(L)]ClO_4 \cdot 0.5DMF$ with atom-numbering scheme.

Table 2. Selected Bond Distances (Å) and Angles (deg) for $[CoCu(L)]ClO_4 \cdot 0.5DMF$

Bond Distances			
Co−O(1)	1.874(3)	Co−O(2)	1.860(3)
Co−N(1)	1.866(4)	Co−N(2)	1.867(4)
Cu−O(1)	2.331(3)	Cu−O(2)	2.384(3)
Cu−N(3)	1.978(4)	Cu−N(4)	1.987(4)
Cu···S	3.075(1)	Cu···Co	3.355(7)
Bond Angles			
O(1)−Co−O(2)	85.7(1)	O(1)−Co−N(1)	94.8(1)
O(1)−Co−N(2)	179.5(1)	O(2)−Co−N(1)	179.5(1)
O(2)−Co−N(2)	94.2(1)	N(1)−Co−N(2)	85.3(1)
O(1)−Cu−O(2)	65.2(1)	O(1)−Cu−N(3)	144.3(1)
O(1)−Cu−N(4)	85.4(1)	O(2)−Cu−N(3)	81.4(1)
O(2)−Cu−N(4)	150.4(1)	N(3)−Cu−N(4)	128.0(1)
Cu−O(1)−Co	105.3(1)	Cu−O(2)−Co	104.3(1)

The $Co^{II}Cu^{I}$ and $Co^{II}Pb^{II}$ complexes have a molar conductivity of 58 and 106 S cm^2 mol^{-1}, respectivity, in DMF, indicating that the former behaves as a 1:1 electrolyte and the latter as a 2:1 electrolyte.[18] All of the complexes show an IR band near 1620 cm^{-1} due to the ν(C═N) mode of the azomethine group. The $Co^{II}Pb^{II}$ complex, $[CoPb(L)(DMF)_2](ClO_4)_2$, shows an IR band at 1649 cm^{-1} attributable to the ν(C═O) mode of the DMF molecule. The perchlorate ν_3 vibration of $[CoPb(L)](ClO_4)_2$ is split into two (1110 and 1060 cm^{-1}), suggesting unidentate function of the group.[19] The corresponding band for the di-DMF adduct, $[CoPb(L)(DMF)_2](ClO_4)_2$, shows no appreciable splitting in accord with the coordination of the DMF molecules instead of perchlorate groups (see below). The Co^{II} is of low spin in both the $Co^{II}Cu^{I}$ and $Co^{II}Pb^{II}$ complexes as evidenced by EPR studies (see Oxygenation Behavior).

Crystal Structures. $[Co^{II}Cu^{I}(L)]ClO_4 \cdot 0.5DMF$. An ORTEP[20] view of the cationic part is shown in Figure 1 together with the atom-numbering scheme. Selected bond distances and angles are given in Table 2.

The result clearly demonstrates that the Co^{II} resides in the salen-like N_2O_2 site and the Cu^{I} in the N_2O_2S site. The perchlorate group and the DMF molecule are free from coordination and are captured in the crystal lattice. The Co--

(13) Cromer, D. T.; Waber, J. T. *International Tables for X-ray Crystallography*; Kynoch Press: Birmingham, 1974; Vol. IV.
(14) Ibers, J. A.; Hamilton, W. C. *Acta Crystallogr.* **1964**, *17*, 781.
(15) Creagh, D. C.; McAuley, W. J. In *International Tables for Crystallography*; Wilson, A. J. C., Ed.; Kluwer Academic Publishers: Boston, 1992; pp 219−222.
(16) Creagh, D. C.; Hubbell, J. H. In *International Tables for Crystallography*; Wilson, A. J. C., Ed.; Kluwer Academic Publishers: Boston, 1992; pp 200−206.
(17) *TEXSAN*; Molecular Structure Corporation: Houston, TX, 1985.
(18) Geary, J. H. *Coord. Chem. Rev.* **1971**, *7*, 81.
(19) Nakamoto, K. *Infrared Spectra of Inorganic and Coordination Compounds*, 2nd ed.; John Wiley & Sons: New York, 1963; pp 175−176.
(20) Johnson, C. K. Report 3794; Oak Ridge National Laboratory: Oak Ridge, TN, 1965.

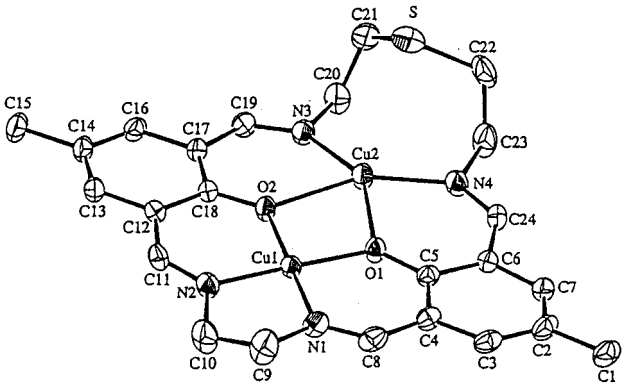

Figure 2. ORTEP view of $[Cu^{II}Cu^{I}(L)]ClO_4 \cdot 0.5DMF$ with atom-numbering scheme.

Cu intermetallic separation bridged by the two phenolic oxygens is 3.355(1) Å. The Co has a planar geometry with the Co−O and Co−N bond distances ranging from 1.860(3) to 1.874(3) Å. The bond distances are comparable to those of Co(salen).[21] The ethylene chain combining the two imine nitrogens assumes the usual gauche conformation.

The Cu^{I} in the N_2O_2S site has a planar four-coordinate geometry with two phenolic oxygens (O1 and O2) and two imine nitrogens (N3 and N4). The thioether atom on the lateral chain is located at an axial site of the Cu^{I} but the Cu--S separation (3.075(1) Å) is too large to be considered as a coordination bond. The Cu is displaced by 0.106 Å from the least-squares plane toward the sulfur. It must be emphasized that the configuration of the $\{CuN_2O_2\}$ chromophore is largely distorted from a regular square. The Cu−O(1) and Cu−O(2) bond distances are considerably long (2.331(3) and 2.384(3) Å, respectively), whereas the Cu−N(3) and Cu−N(4) bond distances are short (1.978(4) and 1.987(4) Å, respectively). Further, the N(3)−Cu−N(4) angle is very large (128.0(1)°), whereas the O(1)−Cu−O(2) angle is small (65.2(1)°). The O(1)−Cu−N(4) and O(2)−Cu−N(3) angles are common (85.4(2)° and 81.42(1)°). Tetrahedral stereochemistry generally predominates for Cu^{I} complexes, but other geometries occur to a limited extent when ligand constraints are favorable.[22] If the elongated Cu−O(1) and Cu−O(2) bonds are assumed to be one coordination bond, the geometry about the Cu^{I} is regarded as a triangle. Such triangular Cu^{I} complexes are commonly known.[23]

$[Cu^{II}Cu^{I}(L)]ClO_4 \cdot 0.5DMF$. An ORTEP view is given in Figure 2 together with the atom-numbering scheme. The selected bond distances and angles are given in Table 3.

The X-ray crystallography has proved that the $Cu^{II}Cu^{I}$ complex has a dinuclear core similar to that for the $Co^{II}Cu^{I}$ complex. The Cu^{II}--Cu^{I} intermetallic separation bridged by the phenolic oxygens is 3.364(1) Å. The Cu^{II} (Cu1) in the N_2O_2 site has an essentially planar geometry with the Cu-to-donor bond distances ranging from 1.895(4) to 1.930(5) Å. The bond distances are comparable to those of Cu(salen).[21] The geometry about the Cu^{I} (Cu2) shows unique distortions as found for the $Co^{II}Cu^{I}$ complex. The Cu(2)−O(1) and Cu(2)−O(2) bond distances are considerably elongated (2.354(3) and 2.386(4) Å, respectively) relative to the Cu(2)−N(3) and Cu(2)−N(4) bond distances (1.993(4) and 1.988(4) Å, respectively). Further, the N(3)−Cu(2)−N(4) angle is large (128.6(2)°), whereas the O(1)−Cu(2)−O(2) angle is small (66.8(1)°). The thioether atom on the lateral chain is positioned at an axial site of the Cu^{I}, but the Cu--S separation is very large (3.011(2) Å).

Table 3. Selected Bond Distances (Å) and Angles (deg) for $[Cu^{II}Cu^{I}(L)]ClO_4 \cdot 0.5DMF$

Bond Distances			
Cu(1)−O(1)	1.913(3)	Cu(1)−O(2)	1.895(4)
Cu(1)−N(1)	1.930(5)	Cu(1)−N(2)	1.929(4)
Cu(2)−O(1)	2.354(3)	Cu(2)−O(2)	2.386(4)
Cu(2)−N(3)	1.993(4)	Cu(2)−N(4)	1.988(4)
Cu(2)···S	3.011(2)	Cu(1)···Cu(2)	3.364(1)
Bond Angles			
O(1)−Cu(1)−O(2)	86.5(1)	O(1)−Cu(1)−N(1)	94.3(2)
O(1)−Cu(1)−N(2)	178.6(2)	O(2)−Cu(1)−N(1)	179.2(2)
O(2)−Cu(1)−N(2)	94.8(2)	N(1)−Cu(1)−N(2)	84.4(2)
O(1)−Cu(2)−O(2)	66.8(1)	O(1)−Cu(2)−N(3)	147.4(2)
O(1)−Cu(2)−N(4)	82.9(1)	O(2)−Cu(2)−N(3)	81.1(1)
O(2)−Cu(2)−N(4)	149.7(2)	N(3)−Cu(2)−N(4)	128.6(2)
Cu(1)−O(1)−Cu(2)	103.6(1)	Cu(1)−O(2)−Cu(2)	103.0(1)

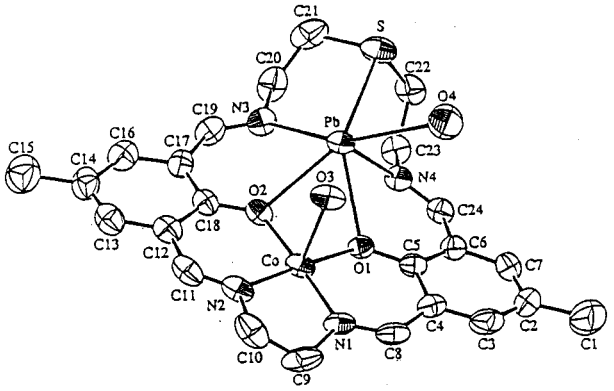

Figure 3. ORTEP view of $[CoPb(L)(DMF)_2](ClO_4)_2$ with atom-numbering scheme.

Table 4. Selected Bond Distances (Å) and Angles (deg) for $[CoPb(L)(DMF)_2](ClO_4)_2$

Bond Distances			
Co−O(1)	1.894(4)	Co−O(2)	1.907(4)
Co−O(3)	2.186(4)	Co−N(1)	1.859(5)
Co−N(2)	1.862(5)	Pb−O(1)	2.557(4)
Pb−O(2)	2.557(4)	Pb−O(4)	2.672(6)
Pb−N(3)	2.593(6)	Pb−N(4)	2.530(5)
Pb···S	3.003(2)	Pb···Co	3.3721(9)
Bond Angles			
O(1)−Co−O(2)	84.6(2)	O(1)−Co−O(3)	89.0(2)
O(1)−Co−N(1)	94.2(2)	O(1)−Co−N(2)	173.5(2)
O(2)−Co−O(3)	88.8(2)	O(2)−Co−N(1)	173.9(2)
O(2)−Co−N(2)	93.8(2)	N(1)−Co−N(2)	87.4(2)
O(1) −Pb−O(2)	60.0(1)	O(1)−Pb−O(4)	88.5(2)
O(1)−Pb−N(3)	112.5(2)	O(1)−Pb−N(4)	68.0(1)
O(2)−Pb−O(4)	139.6(2)	O(2)−Pb−N(3)	71.1(2)
O(2)−Pb−N(4)	106.9(1)	O(4)−Pb−N(3)	149.1(2)
O(4)−Pb−N(4)	80.2(2)		
Pb−O(1)−Co	97.4(2)	Pb−O(2)−Co	97.0(2)

$[CoPb(L)(DMF)_2](ClO_4)_2$. An ORTEP view is shown in Figure 3 together with the atom-numbering scheme. The selected bond distances and angles are given in Table 4.

The Co resides in the N_2O_2 site and the Pb in the N_2O_2S site; the Co--Pb intermetallic separation is 3.37 Å. The Co has

(21) Calligaris, M.; Nardin, G.; Randaccio, L. *Coord. Chem. Rev.* **1972**, *7*, 385.
(22) Hathaway, B. J. *Comprehensive Coordination Chemistry*; Pergamon: Oxford, 1987; Vol. *5*, pp 533−593.
(23) For example: (a) Kappenstein, C.; Hugel, R. P. *Inorg. Chem.* **1978**, *17*, 1945. (b) Weininger, M. S.; Hunt, G. W.; Amma, E. L. J. *J. Chem. Soc., Chem. Commun.* **1980**, 2993. (c) Coucouvanis, D.; Murphy, C. N.; Konadia, S. K. *Inorg. Chem.* **1980**, *19*, 2993.

a square-pyramidal geometry with a DMF oxygen at the axial site. The in-plane bond distances range from 1.859(5) to 1.907(4) Å. The axial Co−O(3) bond distance is longer (2.186(4) Å). The Co is displaced by 0.102 Å from the basal least-squares plane toward the axial DMF oxygen.

The Pb in the N_2O_2S site has apparently a six-coordinate geometry along with a DMF oxygen. The Pb−S bond distance is 3.003(2) Å, and other Pb−N and Pb−O bond distances fall in the range 2.530(5)−2.672(6) Å. It is noticed that the DMF oxygen O(3) at the axial site of the Co forms a bridge to the Pb in the Pb--O(3) interatomic separation of 3.018(4) Å. Thus, the geometry about the Pb can be regarded as a seven-coordination. Such a bridge of the axial donor atom to the adjacent Pb has been found for related $Co^{II}Pb^{II}$ and $Co^{III}Pb^{II}$ complexes.[10a,e,24,25]

Electrochemical Properties. Electrochemical properties of $[CoCu(L)]ClO_4 \cdot 0.5DMF$ were studied in DMF by means of cyclic voltammetry in comparison with $[Cu^{II}Cu^{I}(L)]ClO_4$ and $[CoPb(L)](ClO_4)_2$. The CV of the $Co^{II}Cu^{I}$ complex has two reversible couples at −1.30 and −0.25 V vs Ag/Ag^+. The former can be attributed to the Co^{I}/Co^{II} process.[11,12] The Co^{II}/Co^{III} process for relating macrocyclic $Co^{II}M^{II}$ complexes occurs at ∼−0.3 V (vs Ag/Ag^+) in DMF.[11,12] The $Cu^{II}Cu^{I}$ complex under the same conditions has a reversible couple at −0.26 V attributable to the Cu^{I}/Cu^{II} process in the N_2O_2S site.[8] Thus, it is not straightforward if the couple at −0.25 V of the $Co^{II}Cu^{I}$ complex arises from the oxidation of the Co^{II} center or the oxidation of the Cu^{I} center. In order to make an unambiguous assignment of the couple, controlled-potential electrolyses were done at −0.25 V to indicate one electron transfer. The electrolyzed solution became greenish brown and showed an absorption at 600 nm (ϵ: ∼140 M^{-1} cm^{-1}) that is typical of a planar Cu^{II} chromophore. Thus, the couple at −0.25 V is assigned to the Cu^{I}/Cu^{II} process at the N_2O_2S site. It must be mentioned that the weak Cu--S interaction certainly contributes to the stabilization of Cu^{I}; the Cu^{I}/Cu^{II} potential is negatively shifted by ca. 0.4 V when the thioether sulfur in the lateral chain is replaced by amino nitrogen.[8]

The $Cu^{II}Cu^{I}$ complex has another pseudoreversible couple at −1.37 V that is assigned to the Cu^{I}/Cu^{II} process at the N_2O_2 site.[7a] The $Co^{II}Pb^{II}$ complex in acetonitrile has a reversible couple at −1.02 V and a quasireversible couple at +0.22 V, which are attributed to the Co^{I}/Co^{II} and Co^{II}/Co^{III} processes, respectively.[12] Thus, the $Co^{II}Cu^{I}$ and $Cu^{II}Cu^{I}$ complexes show the Cu^{I}/Cu^{II} process in the N_2O_2S site at similar potentials (−0.25 and −0.26 V, respectively), whereas the $Co^{II}Cu^{I}$ and $Co^{II}Pb^{II}$ complexes show the Co^{I}/Co^{II} process at different potentials (−1.30 and −1.02 V, respectively). The Co^{II}/Co^{III} process of the $Co^{II}Cu^{I}$ complex is irreversible and shows only an anodic peak at ∼+0.8 V.

Oxygenation Behavior. The reactivity of the $Co^{II}Cu^{I}$ complex toward dioxygen was examined in DMF by means of visible spectroscopy. A DMF solution of the complex under anaerobic conditions assumes a red color and shows an intense absorption band at ∼360 nm (ϵ: ∼11800 M^{-1} cm^{-1}) and two moderately intense bands at ∼440 (shoulder) and ∼540 nm (ϵ: ∼1200 M^{-1} cm^{-1}) (Figure 4, trace a). The former intense band is assigned to the $\pi-\pi^*$ transition associated with the azomethine linkage.[26] The two visible bands can be assigned to the LMCT bands from the filled p_π orbital of the phenolic oxygen

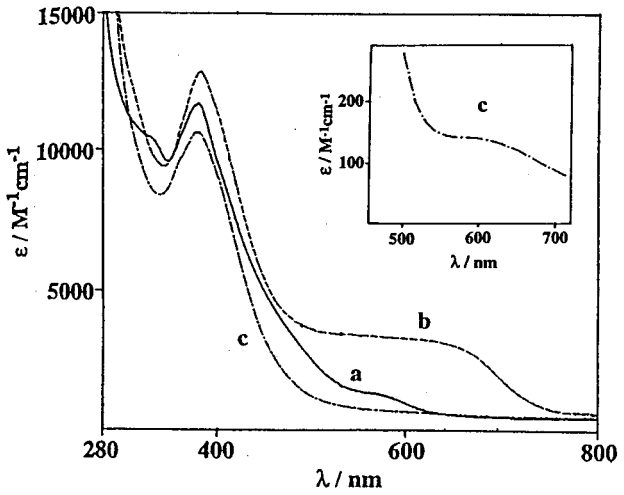

Figure 4. Visible spectra (in DMF) of (a) $[CoCu(L)]ClO_4$ (at room temperature), (b) its oxygenated dark brown solution (at −50 °C, soon after oxygenation), and (c) oxidized yellowish brown solution (3 min after oxygenation). The inset is an expansion of trace c.

to the Co^{II}.[12] When the solution was exposed to dioxygen at −30 °C, an immediate color change occurred from red to pale brown. This is regarded as oxidation of the $Co^{II}Cu^{I}$ complex with dioxygen. At −50 °C, the oxidation was significantly slowed to allow for spectroscopic studies of the oxygenated solution. Soon after exposure to dioxygen at −50 °C, the solution assumed a dark brown color and showed a spectral enhancement in the region of 500−670 nm (trace b). In the oxygenation of analogous $Co^{II}M^{II}$ complexes,[10,11] a μ-peroxo dimer with the $Co^{III}-O-O-Co^{III}$ linkage is predominantly produced irrespective of the nature of the adjacent M^{II} ion. The μ-peroxo dimers are characterized by a LMCT band at ∼550 nm (ϵ ∼2000 M^{-1} cm^{-1}). Such a μ-peroxo dimer must be formed in the oxygenation of the $Co^{II}Cu^{I}$ complex, judged from a discernible absorption near 550 nm in trace b. The most notable feature in trace b is the absorption at the longer wavelength (∼630 nm), indicating the presence of another type of oxygenated species in the solution. The dark brown color of the solution faded to pale brown within 3 min, and the solution showed no prominent absorption in the visible region (trace c) except for a weak band at ∼600 nm attributable to Cu^{II} (see inset). Our resonance Raman spectroscopic studies could not make any confidential assignment of ν(O−O) and ν(M−O) vibrations for the oxygenated species.

The oxidation of the $Co^{II}Cu^{I}$ complex with dioxygen was followed by EPR spectroscopy in frozen DMF at liquid nitrogen temperature (Figure 5). Under anaerobic conditions, the complex solution showed the EPR spectrum of trace a, which is typical of low-spin Co^{II} having one unpaired electron on the d_{z^2}-character orbital.[27] When the frozen solution was exposed to dioxygen, new EPR signals arising from isolated Cu^{II} [28] were superposed on the Co^{II} signals (trace b). The Co^{II} EPR signals became weaker with time (trace c) and were finally replaced with the Cu^{II} signals (trace d). The result clearly demonstrates the oxidation of the $Co^{II}Cu^{I}$ complex into a Co^{III}-Cu^{II} complex with dioxygen. EPR signals attributable to superoxo cobalt complex could not be detected in traces b and c.

(24) Furutachi, H.; Ōkawa, H. *Bull. Chem. Soc. Jpn.* **1998**, *71*, 671.
(25) Costa, G.; Puxeddu, A.; Bardin, S. L. *Inorg. Nucl. Chem. Lett.* **1970**, *6*, 191.
(26) Bosnich, B. *J. Am. Chem. Soc.* **1968**, *90*, 627.
(27) Nishida, Y.; Kida, S. *Coord. Chem. Rev.* **1979**, *27*, 275.
(28) Goodman, B. A.; Raynor, J. B. *Adv. Inorg. Chem. Radiochem.* **1970**, *13*, 135.

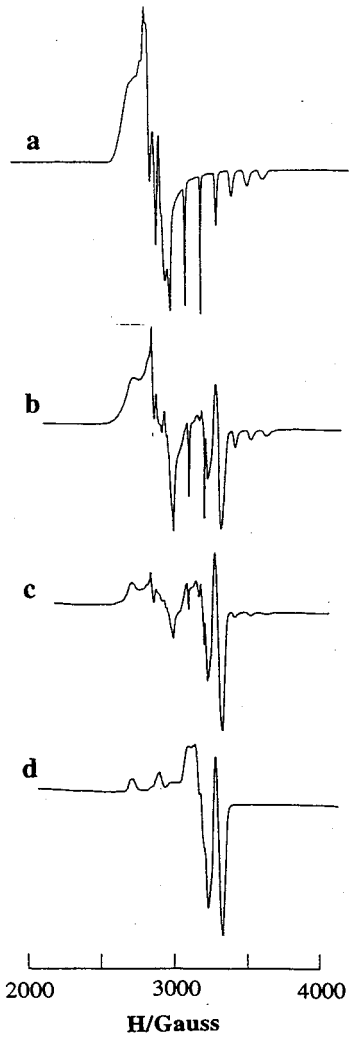

Figure 5. EPR spectra (at 77.4 K) of (a) a frozen DMF solution of $[CoCu(L)]ClO_4$ and its oxidized solutions with dioxygen (b, 10 min; c, 20 min; d, 30 min after exposure to dioxygen).

For comparison, the oxygenation behavior of the $Cu^{II}Pb^{II}$ and $Co^{II}Cu^{I}$ complexes was studied. A red DMF solution of the Co^{II}-Pb^{II} complex exhibits an intense absorption band at ~350 nm and two moderately intense bands at ~430 and ~550 nm under anaerobic conditions. This spectrum resembles that of the Co^{II}-Cu^{I} complex (Figure 4, trace a). When exposed to dioxygen at 0 °C, the solution assumed a dark brown color and showed an absorption around 550 nm (ϵ: 2200 M^{-1} cm^{-1}). This indicates the formation of the peroxo dimer, $Pb^{II}Co^{III}-O-O-Co^{III}$-$Pb^{II}$.[10,11] The deoxygenation was performed when the oxygenated solution was purged with argon or warmed to room temperature. A frozen DMF solution of the $Co^{II}Pb^{II}$ complex showed an EPR spectrum essentially the same as trace a in Figure 5. Upon exposure to dioxygen, the solution became EPR-silent in harmony with the formation of the μ-peroxo dimer. The oxygenation of the $Co^{II}Pb^{II}$ complex is explained by the two successive steps[9-11]

$$[Co^{II}Pb^{II}(L)]^{2+} + O_2 \rightleftharpoons [Co^{III}Pb^{II}(L)(O_2^{-})]^{2+}$$

$$[Co^{III}Pb^{II}(L)(O_2^{-})]^{2+} + [Co^{II}Pb^{II}(L)]^{2+} \rightleftharpoons [\{Co^{III}Pb^{II}(L)\}_2(O_2^{2-})]^{4+}$$

The dominant oxygenated species in the solution is the μ-peroxo dimer $[\{Co^{III}Pb^{II}(L)\}_2(O_2^{2-})]^{4+}$ as proved for analogous $Co^{II}M^{II}$ complexes,[10,11] since no EPR signal attributable to superoxo cobalt complex[9] is detected in traces b and c. It must be mentioned that Co(salen) and analogous Schiff-base Co^{II} complexes form predominantly the superoxo complex.[9] The Cu^{II}-Cu^{I} complex was inert to dioxygen even at −50 °C.

Scheme 1. Oxygenation of $[CoCu(L)]ClO_4$ and $[CoPb(L)](ClO_4)_2$

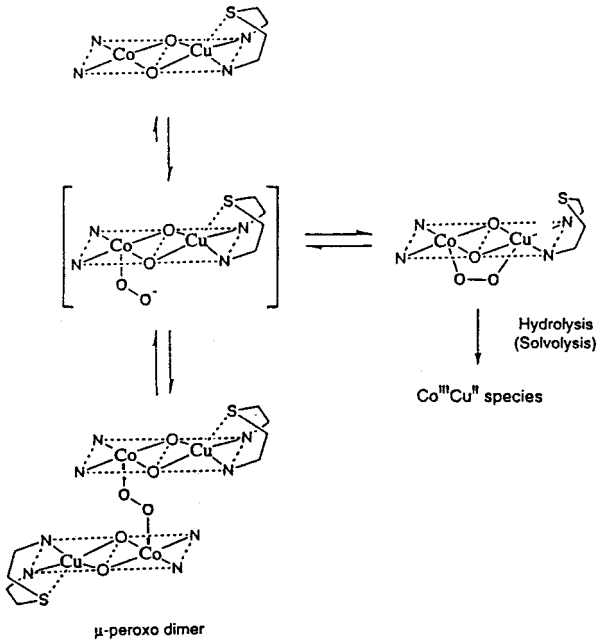

Thus, it is obvious that the $Co^{II}Cu^{I}$ complex is exceptionally reactive toward dioxygen so as to be converted into a $Co^{III}Cu^{II}$ species. This fact strongly suggests an interplay of the Co^{II} and Cu^{I} ions in the oxygenation providing an intramolecular μ-peroxo complex, $[Co^{III}Cu^{II}(L)(O_2^{2-})]^{+}$.[10e,11] The absorption transiently observed near 630 nm (Figure 4, trace b) must be associated with the peroxo complex. In general peroxo dicopper(II) complexes have the peroxo-to-Cu^{II} LMCT band at 525 ~ 545 nm,[29] but this band shifts to a longer wavelength when the geometry about the Cu is distorted.[30] The X-ray crystallographic study for the $Co^{II}Cu^{I}$ complex has revealed an unusual geometry about the Cu (Figure 1). We presume that the Cu^{II} in the intramolecular peroxo complex has a largely distorted geometry so that the peroxo-to-Cu^{II} LMCT band appears at longer wavelength (~630 nm). The intramolecular peroxo complex must be equilibrated with the peroxo dimer $[\{Co^{III}Cu^{I}(L)\}_2(O_2^{2-})]^{4+}$ through the superoxo cobalt complex, $[Co^{III}Cu^{I}(L)(O_2^{-})]^{+}$. The oxygenation of the $Co^{II}Cu^{I}$ complex is schematically shown in Scheme 1.

Porphinato−Fe^{II} and −Co^{II} complexes having a Cu(I) auxiliary were prepared as models of the heme a_3/Cu_B center,[31,32] and the stable dioxygen adducts, $Fe^{III}-O_2^{2-}-Cu^{II}$, were derived from these complexes. Thus, the unstability of the intramolecular μ-peroxo species of the $Co^{II}Cu^{I}$ complex is notable. It appears that the oxidation of the Cu^{I} accompanies a

(29) Karlin, K. D.; Kaderli, S.; Zuberbühler, A. D. *Acc. Chem. Res.* **1997**, *30* , 139.
(30) Becker, M.; Heinemann, F. W.; Schindler, S. *Chem.—Eur. J.* **1999**, *5*, 3124.
(31) (a) Collman, J. P. *Inorg. Chem.* **1997**, *30*, 5145. (b) Collman, J. P.; Fu, L.; Herrmann, P. C.; Zhang, X. *Science* **1997**, *275*, 945. (c) Collman, J. P.; Fu, L.; Herrmann, P. C.; Wang, Z.; Rapta, M.; Broring, M.; Schwenninger, R.; Boitrel, B. *Angew. Chem., Int. Ed.* **1998**, *37*, 3397. (d) Collman, J. P.; Schwenninger, R.; Rapta, M.; Broring, M.; Fu, L. *Chem. Commun.* **1999**, 137.
(32) Sasaki, T.; Nakamura, N.; Naruta, Y. *Chem. Lett.* **1998**, 351.

large configurational change about the metal, from the distorted $\{Cu^{I}N_2O_2\}$ in Figure 1 to a planar $\{Cu^{II}N_2O_2\}$ with the usual bond distances and angles, and that this facilitates the hydrolytic (or solvolytic) replacement of the peroxo group.

Acknowledgment. This work was supported by Grants-in-Aid for Scientific Research (No. 09440231), Scientific Research on Priority Area "Metal-assembled Complexes" (No. 10149106), and an International Scientific Research Program (No. 09044093) from the Ministry of Education, Science and Culture, Japan.

Supporting Information Available: Positional and thermal parameters of non-hydrogen atoms and full bond distances and angles for the $Co^{II}Cu^{I}$, $Cu^{II}Cu^{I}$, and $Co^{II}Pb^{II}$ complexes in CIF format. This material is available free of charge via the Internet at http://pubs.acs.org.

IC000305E